acta phys. slov. 34 (1984), No. 1

ON THE LIMITS TO FUSION IN THE $^{20}Ne+^{40}Ca$ SYSTEM

M. M. SHALABY[1]), Y. EL-DEGHEIDY[2]), M. M. KHALIL[1]), N. MORGAN[1]), Cairo

Diffraction model analysis of $^{20}Ne+^{40}Ca$ elastic scattering data (44.1 MeV$\leq E_{lab}\leq$151 MeV) is performed to determine the cut-off orbital angular momentum (L_c) and the total reaction cross section. A Fermi function type for the fusion probability was proposed and used in a partial wave expansion for calculating the fusion cross section ($\sigma_{fus}(E)$). The derived fusion angular momentum (L_f) together with L_c could explain the observed saturation limit of $\sigma_{fus}(E)$ as a transition in motion from (nearly) rolling to sticking friction. Also the limit of $\sigma_{fus}(E)$ could be attributed to the "statistical yrast line" of the corresponding compund nucleus. A rough estimate for the energy loss associated with reduction of L_c to L_f is given.

О ПРЕДЕЛАХ СИНТЕЗА СИСТЕМЫ $^{20}Ne+^{40}Ca$

В работе представлены результаты анализа данных об упругом рассеянии (44,1 МэВ$\leq E_{lab}\leq$151 МэВ) в системе $^{20}Ne+^{40}Ca$ на основе дифракционной модели с целью определения параметра обрезания для орбитального углового момента (L_c) и полного поперечного сечения реакции. В разложении по парциальным волнам для вычисления поперечного сечения синтеза ($\sigma_{fus}(E)$) предложены и использованы для вероятности синтеза функции типа Ферми. Определенный угловой момент синтеза (L_f) сместе с L_c могут объяснить наблюдаемый предел насыщения $\sigma_{fus}(E)$ как изменение в характере движения от (почти) трения качения к трению слипания. Предел $\sigma_{fus}(E)$ может быть также приписан «статистической ираст-линии» соответствующего компаунд-ядра. Приведено также приближенное вычисление энергетических потерь, связанных с сведением L_c к L_f.

I. INTRODUCTION

Different approaches were proposed for the limitation of the fusion cross section ($\sigma_{fus}(E)$) in light-heavy ion-systems at high energies. Harar [1] suggested that the fusion limiting mechanism could be due to an angular momentum limitation imposed by the properties of the compound nucleus. Kolata [2] attributed this

---

[1]) Physics Dept. Fac. of Science, Ain Shams University, CAIRO, Egypt.

[2]) El-Mansora University, El-MANSORA, Egypt.

limitation in some way to properties of the compound system and that its onset was more violent than previously suspected. On the other hand deformation and shell effects, included in determining an yrast line cannot be responsible for the observed drop of σ_{fus} below σ_T [3]. Lee et al. [4] introduced a "*statistical yrast line*" that lies parallel to the usual (compound nucleus) yrast line, but is shifted upward by an additional energy ΔQ; to account for fusion cross section limitation. It is based on the arguments that fusion is appreciable for a given partial wave (L_f) if the compound system energy lies at or above the region where the level density is reasonably high. This approach successfully accounted for limits in $\sigma_{fus}(E)$ for several systems (with $A \leq 80$) as $C^{12}+B^{11}$ [5] and $O^{16}+Si^{30}$ [6]. The fusion limit in other systems as $C^{13}+B^{11}$ [5] and $O^{16}+Ca^{40}$?7] has not been satisfactorily explained in terms of the "*statistical yrast line*" of the corresponding compound nuclei (Na^{23} and Ni^{56}, respectively) and it was generally attributed to entrance channel characteristics.

In data for the fusion energy excitation function of the light-heavy ion system $Ne^{20}+Ca^{40}$ [8, 9] over the energy range of 40—70 MeV and at 151 MeV a limitation of $\sigma_{fus}(E)$ was observed at $E_{lab} = 151$ MeV and represents about half of the corresponding total reaction cross section. The present work is an attempt to attribute this observation to: (i) the reduction in the entrance channel angular momentum due to tangential friction. (ii) the "*statistical yrast line*" limit of the corresponding compound nucleus (Zn^{60}). The $Ne^{20}+Ca^{40}$ data set was chosen as it includes both elastic scattering and fusion cross sections to determine L_c and L_f, respectively, over a wide range of energies.

II. METHOD OF ANALYSIS

We outline here a direct method for extracting the critical angular momentum L_{crit} (for fusion), referred here to as (L_f) and the cut-off angular momentum (L_c). It is based on the diffraction model analysis of elastic scattering data (to determine T_l and L_c) and the partial wave expansion for the fusion cross section assuming a Fermi function type for the fusion probability $P_l^{(f)}$ (to determine L_f).

To calculate the elastic scattering cross section we use the formula $d\sigma/d\Omega = f(\Theta)^2$, where the amplitude for the elastic scattering $f(\Theta)$ is given by

$$f(\Theta) = f_c(\Theta) + \frac{i}{2K} \sum_{l=0}^{\infty} (2l+1) e^{2i\sigma_l} (1 - S_l) P_l(\cos\Theta) \qquad (1)$$

where $f_c(\Theta)$ is the Rutherford elastic scattering amplitude, σ_l are the pure Coulomb phase shifts and S_l are the nuclear diagonal S matrix elements. They are taken to have the smooth S shape rise to unity as a function of l:

$$S_l = (1 + e^{-i\alpha} \exp[(L_c - l)/\Delta])^{-1}, \qquad (2)$$

it is centred at the cut-off orbital angular momentum L_c with the total width Δ, and α is a parameter giving a non-vanishing real part to the phase shift [10]. These parameters were used as adjustable parameters to fit the $^{20}Ne + ^{40}Ca$ elastic scattering data over the energy range 44.1 MeV $\leq E_{lab} \leq$ 151 MeV (Fig. 1) with parameters given in Table 1.

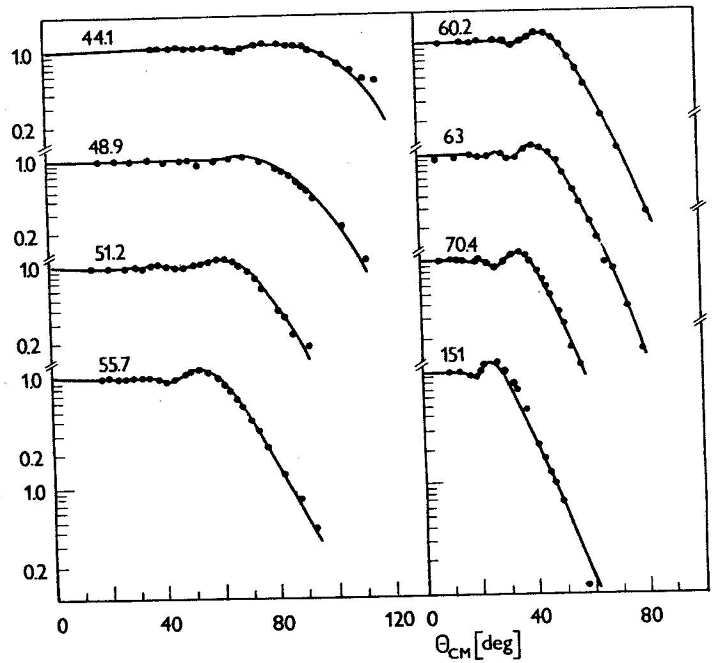

Fig. 1. Elastic scattering analysis of $^{20}Ne + ^{40}Ca$ at $E = 44.1$—151 MeV. Experimental data are of Van Sen et al. [8] [9]. Full curves indicate the diffraction model analysis with parameters given in Table 1.

In the analysis of the $^{20}Ne + ^{40}Ca$ fusion data we consider a partial wave expansion for the reaction cross section:

$$\sigma_{fus}(E) = \frac{\pi}{K^2} \sum_l (2l+1) P_l^{(f)} T_l \qquad (3)$$

where T_l is the diffraction model transmission coefficient; $T_l = (1 - |S_l|^2)$ and $P_l^{(f)}$ is the probability that the system will emerge in the fusion channel. We first set $P_l^{(f)}$ equal to unity and derive values of the diffraction model total reaction cross sections σ_T (Fig. 2). These values are in full agreement with those obtained from the optical model analysis [8, 9], which presents a justification for the derived

Table 1

Diffraction model parameters for ^{20}Ne + ^{40}Ca (a). Cutt-off angular momentum (L_c) and total reaction cross section (σ_T) are deduced from elastic scattering fits. Fusion angular momenta (L_f) are deduced from fitting σ_{fus} (equations 3, 4) to the experimental fusion excitation function.

E_{lab} (MeV)	L_c	σ_T (mb)	L_f	ΔE (MeV)$^{(b)}$
44.1	11	319	9	1.08
48.9	16	557	14	1.50
51.2	20	762	17	2.93
55.7	24	929	21	3.55
60.2	28	1138	24	5.44
63	30	1234	26	5.86
70.4	35	1431	31	6.89
151	68	2428	45	40.00

(a) The parameters Δ and α are taken 1.5 and 0.5, respectively, except at $E_{lab} = 151$ MeV where they are 2.6 and 0.9.
(b) ΔE values derived using $\langle R \rangle = 7.9$ fm, except at 151 MeV; $\langle R \rangle$ is 10.2 fm.

diffraction model parameters and in particular values of L_c. To calculate the fusion probability $P_l^{(f)}$, Glass and Mosel [11] have introduced a sharp angular momentum cut-off for $P_l^{(f)}$:

$$P_l^{(f)} = \begin{cases} 1 & \text{for } l \leq L_f \\ 0 & \text{for } l > L_f \end{cases}$$

where L_f is the largest angular momentum for which fusion takes place. On the other hand a critical angular momentum for fusion was defined in a sharp cut-off approach [2] as

$$T_l P_l^{(f)} = \begin{cases} 1 & \text{for } l \leq l_f \\ 0 & \text{for } l > L_f \end{cases}.$$

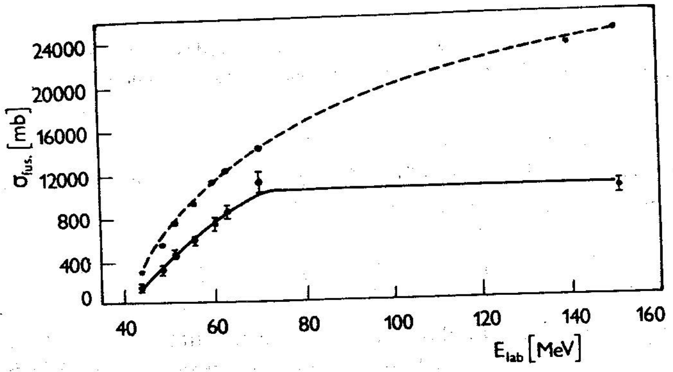

Fig. 2. Fusion excitation function compared to theoretical calculations. Experimental data are of Van Sen et al. [8, 9]. —— σ_{fus} calculated using equations (3) and (4). – – – diffraction model total reaction cross section; . . . . optical model total reaction cross section.

We assume a more realistic smooth variation of $P_l^{(f)}$ instead of the rectangular shape, in which partial waves $< L_f$ are almost completely fused while those with $L_f \leq l < L_c$ do not fuse (completely) and are distributed over several direct reaction channels. The following Fermi shape for $P_l^{(f)}$ was used;

$$P_l^{(f)} = (1 + \exp[(l - L_f)/\Delta])^{-1}. \qquad (4)$$

To avoid (any) further parametrization we have taken the same Δ in equations (2) and (4). Equation (3) with $P_l^{(f)}$ as given in (4) was used to fit the fusion energy excitation function and the derived L_f values are given in Table 1. Variations of both L_c and L_f as a function of incident ^{20}Ne energies are shown in Fig. 3.

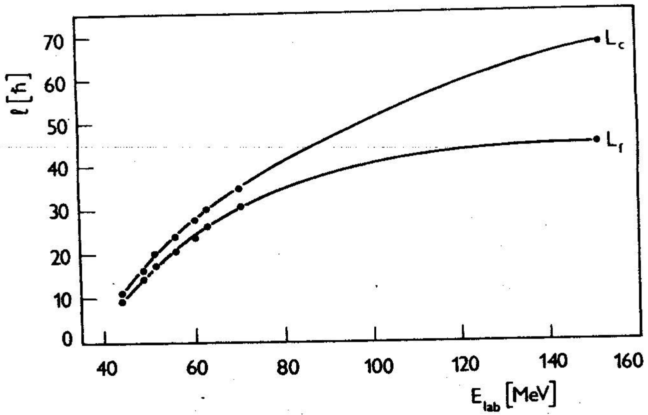

Fig. 3. Variations of cut-off (L_c) and fusion (L_f) orbital angular momenta as a function of incident ^{20}Ne energies.

III. RESULTS AND DISCUSSION

As seen from Table 1 there is a reduction in the entrace channel angular momentum of approximately 0.15 for ^{20}Ne incident energies ≤ 70.4 MeV. This value is lower than that reported by Lefort [12] as 0.28 in his study on the frontier between complete fusion and other dissipative collisions of massive heavy ions (Ar + Ho and Mg + Ta). On the other hand a considerable reduction of $\simeq 0.33$ was observed at the relatively higher incident energy of ^{20}Ne ($E_{lab} = 151$ MeV), possibly describing the transition in motion from (nearly rolling) to sticking motion. It is this reduction due to tangential energy dissipation which is necessary to reproduce a fusion cross section and directly explains its observed saturation limit.

a) *"Statistical yrast line"* limit to fusion.

One of the more recent compound nucleus based models [4] suggested that a *"statistical yrast line"* is responsible for the fusion cross section limitations. From a study of several fusion systems with $A \leqslant 80$ Lee et al. [4] find that this line lies parallel to the usual yrast line but is shifted upward by an additional energy $\Delta Q = 10 \pm 2.5$ MeV. The parameter ΔQ provides an excitation energy above the first level of a given spin at which the level density has become high enough. The excitation energy of the compound nucleus ($E^*_{L_f}$) is expressed as

$$E^*_{L_f} = \frac{\hbar^2}{2J} L_f(L_f+1) + \Delta Q \quad \textit{"statistical yrast line"}$$

or

$$E^*_{L_f} = \frac{\hbar^2}{2J} L_f(L_f+1) \quad \textit{"usual yrast line"}$$

where J is the moment of inertia of the compound nucleus A which is assumed to be equal to that of a rigid rotor $= 2/5\, MR^2$, $R = r_0 A^{1/3}$ and $r_0 = 1.20 \pm 0.05$ fm.

The angular momentum for fusion L_f is plotted in Fig. 4 versus E^* (excitation energy of compound nucleus), $E^* = E_{cm} + Q$ where Q is the ground-state Q value of the entrance channel. Also shown in this figure are the *"statistical yrast line"* calculations (solid curve) and the usual yrast line calculations (dotted curve) with $\Delta Q = 12.5$ MeV and $r_0 = 1.10$ fm (two standard deviations lower than its mean value). Within this statistical uncertainty of the parameter r_0 one can attribute limits in the $Ne^{20} + Ca^{40}$ fusion cross section to the statistical yrast line of the compound Zn^{60} nucleus.

b) Rough estimate for energy loss ΔE.

To have a rough estimate for the associated energy loss ΔE, we use the following equality

$$E_{cm} = V_{coul}(R) + V_{Nucl}(R) + \frac{L_c(L_c+1)\hbar^2}{2\mu R^2}. \qquad (5)$$

A point charge potential was used for the coulomb part: $V_{coul}(R) = Z_I Z_T e^2/R$. The nuclear potential was first taken as the real part of the optical model potential that best fits the elastic scattering data over the energy range 44.1 MeV $\leqslant E_{lab} \leqslant$ 151 MeV [8, 0]

$$V_{nucl} = -63.54 \times \left[1 + \exp\frac{(r - 1.18(A_I^{1/3} + A_T^{1/3}))}{0.68}\right]^{-1}. \qquad (6)$$

As a direct consequence of the presence of a pocket in the effective potential (equation 5) three classical turning points (zeros of $E_{cm} - V(R)$) are identified at each incident E_{cm} energy. The outermost turning point where the nuclear potential is approximately negligible was at $\langle R \rangle = 10.2$ fm. We define a radius of interaction

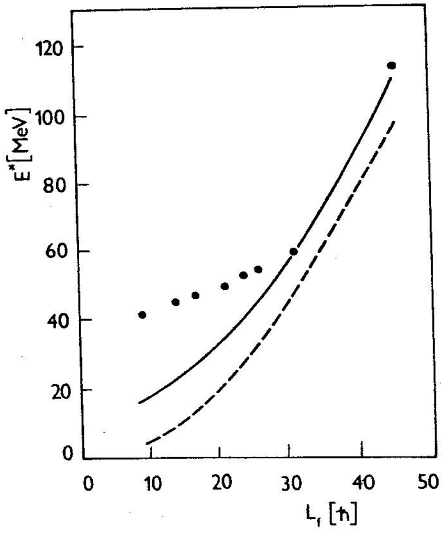

Fig. 4. Fusion angular momentum VS fused system excitation energy. The solid and dashed curves are, respectively, the statistical yrast line and the usual yrast line calculated with the parameters discussed in the text.

R as the middle of the three points at which equation (5) is satisfied. The gradual decrease in R with increasing E_{cm} from 29.4 MeV to 46.9 MeV ($8.7 > R > 7.2$) reflects shrinkage in the strong absorption region with increasing incident energy. The corresponding energy-average radius of interaction $\langle R \rangle$ could be taken as 7.9 fm. This value is almost close to the 7.4 fm calculated from $R = r_0 A_{I,T}^{1/3} - 0{,}76 + 0.8 A_{I,T}^{-1/3}$ [13] and $r_0 = 1.37$ [9]. Two other nuclear potentials were tried, the proximity potential [13] where the range of nuclear forces between two ions is short in comparison with the nuclear dimensions and the SWW potential derived from the liquid drop model [14]. These potentials are found to be less attractive than the real optical model potential, particularly near the nuclear surface, so that the pocket in the total (effective) potential (producing turning points) becomes too shallow more rapidly with increasing energy (increasing L_c values). This limits the possibly extracted $\langle R \rangle$ to much lower energies. At $E_{lab} = 151$ MeV, using the three different nuclear potentials, the pocket completely disappeared ($L_c = 68$) and equation(5) was satisfied at $R = 10.2$ fm. Taking $\langle R \rangle = 7.9$ fm as an effective radius of interaction and substituting it together with L_f instead of L_c into equation (5) the derived values for the energy loss ΔE are given in Table 1. It is to be noted that with the increasing reduction of angular momentum (increasing energy $\leqslant 70.4$ MeV), the centrifugal force is also reduced, hence the number of partial waves which experience a less repulsive interaction at $r \simeq \langle R \rangle$ is increased. However, a saturation limit will be manifested at the relatively higher incident energy (151 MeV) where the pocket becomes shallow ($L_f = 45$) and neither the energy loss ΔE or the reduction in the entrance channel angular momentum ($L_c - L_f$) can compensate for the increasingly repulsive centrifugal potential.

ACKNOWLEDGEMENTS

The authors are highly indebted to Dr. A. El-Naiem and Dr. H. Khalil (University College for Girls, Ain Shams University) for useful suggestions and helpful discussions.

REFERENCES

[1] Harar, S. *Nuclear Molecular Phenomena.* North Holland Amsterdam 1978.
[2] Kolata, J. J.: Phys. Lett. *95 B* (1980), 215.
[3] Mosel, U.: *Proc. of the Internat. Conf. on Nuclear Interactons.* Canberra (Springer) (1978), 185.
[4] Lee, S. M., Matsusa, T., Arima, A.: Phys. Rev. Lett. *45* (1980), 165.
[5] Mateja, J. F., Frawley, A. D., Dennis, L. C., Abdo, K., Kemper, K. W.: Phys. Rev. Lett. *47* (1981), 311.
[6] Chiou, M. S., Wu, M. M., Easwar, N., Maher, J. V.: Phys. Rev. *C 24* (1981), 2507.
[7] Dicenzo, S. B., Petersen, J. F., Betts, R. R.: Phys. Rev. *C 23* (1981), 2561.
[8] Van Sen, N., Darves-Blanc, R., Gondrand, J. C., Merchez, F.: Phys. Rev. *C 20* (1979), 969.
[9] Van Sen, N., Gondrand, J. C., Merchez, F., Darves-Blanc, R.: Phys. Rev. *C 22* (1980), 2424.
[10] Ericson, T. E. O.: *Preludes in Theoretical Physic* North Holland Amsterdam 1965.
[11] Glas, D., Mosel, U.: Nucl. Phys. *A 237* (1975), 429; Phys. Rev. *C 10* (1974), 2620.
[12] Lefort, M.: Zeit. für Phys. *A 299* (1981), 47.
[13] Blocki J., Randrop, J., Swiatecki, W. J., Tsang, C. F.: Ann. Phys. N. Y. *105* (1977), 427.
[14] Siwek-Wilczynska, K., Wilczinski, J.: Phys. Lett. *74 B* (1978), 313; Phys. Lett. *55 B* (1975), 270.

Received January 10th, 1983.